Wave-packet dynamics and quantum beats

B. M. Garraway
Optics Section, The Blackett Laboratory, Imperial College, Prince Consort Road, London SW7 2BZ, United Kingdom
and SCOAP & Centre for Theoretical Physics, CPES, University of Sussex, Falmer, Brighton BN1 9QJ, United Kingdom

K.-A. Suominen
Helsinki Institute of Physics, PL 9, FIN-00014 Helsingin Yliopisto, Finland
and Theoretical Physics Division, Department of Physics, University of Helsinki, PL 9, FIN-00014 Helsingin Yliopisto, Finland
(Received 1 May 1997)

Quantum beats provide a useful tool in spectroscopy for the evaluation of fixed energy level differences. However, in wave-packet dynamics the motion of wave packets about molecular energy surfaces provides time-dependent energy differences. Thus a superposition of wave packets on two excited energy states can yield quantum beats with a time-dependent frequency that depends on the molecular dynamics. We explore this problem with examples and simple models of wave-packet quantum beats. The effects of separating wave packets, and wave packet dispersion, are of especial interest. Calculations are performed using a numerical integration of the time-dependent Schrödinger equation with three energy states and time-dependent couplings. The effects of spontaneous emission are determined by using a fully quantum mechanical Monte Carlo wave-function method. [S1050-2947(98)01807-1]

PACS number(s): 42.50.Md, 33.80.Be, 31.70.Hq

I. INTRODUCTION

The introduction of ultrashort pulses into molecular physics has allowed the exploration of molecules with wave packet dynamics [1,2]. The momentary coupling of two potential energy surfaces introduces a localized wave packet on an excited state. With the coupling gone, this wave packet propagates on the potential surface (as a superposition of vibrational states) and may subsequently be detected using absorption by ultrashort pulses, or time-resolved measurement of fluorescence. The observed wave-packet motion then reveals information about the molecule and its environment, and thus enables, for example, steering of the molecule into a specific state.

This paper focuses on one effect specific to three-state systems subjected to spontaneous emission: wave-packet quantum beats. These systems are an appropriate field of study because the ultrashort pulses used to create excited state wave packets have a broad bandwidth, and may easily excite wave packets on more than one electronic state. If two electronic states are coherently excited then we can expect quantum beats as the excitation decays back to the ground electronic state (see Ref. [3] for the atomic case). The energy difference of the excited-state potential surfaces at the location of the wave packet specifies the beat frequency. Thus in molecules the motion of the wave packet leads to time-dependent variations in the beat frequency and amplitude, which are not present in the atomic case.

We shall consider a model of a molecule with three electronic potential energy surfaces: the ground-state surface U_0 and two excited-state surfaces U_1 and U_2 (see Fig. 1) in a V configuration. We will focus on the usual V configuration though it is possible to obtain quantum beats with ladder systems [4]. We work within the Born-Oppenheimer approximation, and make the rotating wave approximation when we describe the couplings $V_j(t)$ $(j=1,2)$ of the molecular states to a short pulse of light. In many molecules the ground-state potential may be nearly harmonic and thus the corresponding wave function is a good approximation to a Gaussian wave packet. Then a very short pulse of light couples the ground-state wave packet to the excited states. For all but the shortest pulses there will be an uneven redistribution of the packet on the excited states because of the spatially varying detuning [5]. After excitation the coupling is removed and all the wave packets start to move because

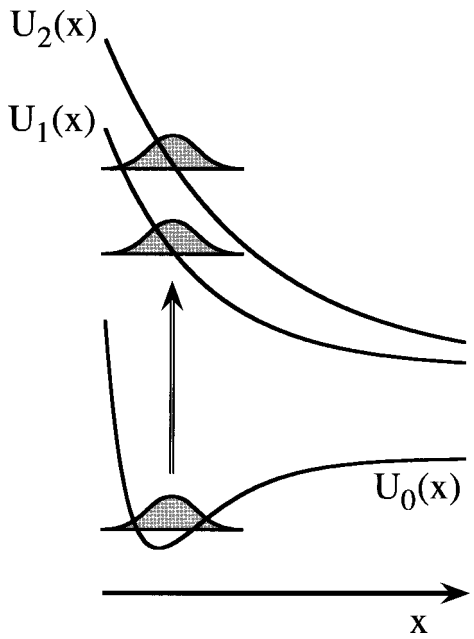

FIG. 1. Three potential energy surfaces $U_j(x)$ illustrated as a function of a molecular coordinate x. The arrow indicates the approximate effect of an ultrashort pulse—to lift parts of the ground state wave packet to the excited states 1 and 2. Specific forms for U_j are given in Sec. IV.

they are not in equilibrium on their surfaces. These motions are on vibrational time scales and may lead to oscillations or dissociation depending on the specific form of the U_j. During the wave-packet motion spontaneous decay causes the excited-state wave packets to return to the ground state; because they have been coherently excited quantum beats may be observed in the fluorescence.

We will present in this paper some model calculations of the quantum beat signal and how it is influenced by the presence of wave-packet dynamics. This will be done in three different ways, including a brute force numerical approach. We will consider only some model three-level systems, ignoring all the complications of additional nearby levels in order to present some of the basic ideas and phenomena, and in order to test some of our algorithms and approximate methods. (Nevertheless, the methods presented can be applied to realistic systems.) In order that the effects of the wave-packet dynamics can be demonstrated, it is essential that the time scale for the decay of the system should be longer than a time scale characterizing the dynamics of the wave packets (e.g., a vibrational time scale). In molecular systems this allows us to use decay, or fluorescence, as a means to monitor the postexcitation wave-packet dynamics, and this has already been achieved experimentally [6]. If the time scale for decay is very long compared to the wave-packet dynamics we will not observe population decay, for example, in a quantum beat signal, if we monitor the system over time scales that are comparable to the wave-packet dynamics. However, we will still observe beating effects if the beat frequency is sufficiently fast. For the model systems in this paper we have chosen decay rates that are not vastly greater than the time scales of the wave-packet dynamics. This allows us to show the population decay, and makes the problem more amenable to the brute force approach. (Nevertheless, for low decay rates, the various methods we describe can still be applied.) The regime where the decay time scale more nearly matches the dynamical time scale arises in an interesting physical situation where spontaneous emission and molecular dynamics couple in cold collisions between laser cooled atoms [7]. The slowly moving atoms form a quasimolecule, which can be excited resonantly during the collision due to the presence of laser light. This can be modeled as a wave-packet process, which is then treated numerically or using semiclassical approximations [8]. So far the time-dependent studies of cold collisions have mainly considered the case of a single excited-state potential surface, but in realistic systems we have a manifold of molecular fine and hyperfine states that do not differ much in energy, especially at large internuclear distances, where the resonant excitation takes place. Thus the discussion of multistate excitation and decay given in this paper is also relevant to the treatment of multistate models of cold collisions, especially when it comes to the methods used to solve the dynamical problem [9].

In the following section we describe the quantum mechanical treatment of the processes leading to quantum beats in molecules. We also describe how to solve the time evolution of wave packets numerically in the presence of spontaneous emission by using a quantum Monte Carlo approach. This method is necessary if information is needed on the ground-state wave-packet dynamics, or if the time scale of the excitation process is sufficiently long that there can be some decay during the preparation of the wave packets. However, if the excitation process is very short, and if we do not need the ground-state information, we can use other, simpler approaches, such as the method using optical potentials discussed in Sec. III (which is based on the textbook [10] approach to quantum beats). We can also make useful approximations by using Gaussian wave packets, and this work is presented in Sec. IV. In Sec. IV we also make a comparison of the methods with some simple examples. The paper is concluded in Sec. V.

II. DENSITY MATRIX FORMULATION

A. Atomic quantum beats

Quantum beats have been used as a tool to study the energy levels in atoms for quite some time [3,11,12] and to exploit the basic phenomenon of quantum interference when there are two possible paths for a quantum system to take. In the atomic system the two paths are simply the routes from the two excited states to the ground state. The quantum beats need to be distinguished from their classical counterpart, which can be seen when two classical waves simply interfere on a photodetector [13].

Using a standard perturbative approach it is possible to write down the master equation for the density matrix of the three-level system undergoing decay [14–16] (and see also [17]):

$$\frac{d}{dt}\rho = -i[H_a,\rho] - \tfrac{1}{2}(J^\dagger J\rho + \rho J^\dagger J - 2J\rho J^\dagger), \tag{1}$$

where the transition operator is

$$J = \sqrt{\gamma_1}\sigma_1^- + \sqrt{\gamma_2}\sigma_2^- . \tag{2}$$

This operator ensures that the emission comes from both transitions. Here $\sqrt{\gamma_j}$, $j=1,2$ represent the dipole matrix elements leading to decay at the rates γ_j, and $\sigma_i^{\pm}$ are the raising $(+)$ and lowering $(-)$ operators that move the system between the excited state j and ground state. For the atomic system the Hamiltonian is simply

$$H_a = \begin{bmatrix} \omega_1 & \Omega_1(t) & 0 \\ \Omega_1(t) & \omega_0 & \Omega_2(t) \\ 0 & \Omega_2(t) & \omega_2 \end{bmatrix}, \tag{3}$$

where ω_0, ω_1, and ω_2 are the frequencies of the transitions between the three levels and Ω_1 and Ω_2 are the time-dependent couplings given in angular momentum units (Rabi frequencies). Here we use a basis such that the total wave function is

$$\Psi_a = \begin{pmatrix} C_1 \\ C_0 \\ C_2 \end{pmatrix}, \tag{4}$$

where the C_j are the time-dependent probability amplitudes of the three states. All the effects of level shifts have been included in the master equation (1) with the appropriate

choice of frequencies ω_j and the decay rates [16]. The master equation (1) also includes the effects of *off-diagonal damping*. The off-diagonal damping terms in the master equation are responsible for a coupling between coherences and populations (i.e., between diagonal and off-diagonal elements of the density matrix). The effects are usually small, unless the energy difference of the two excited states becomes comparable to the spread of energy from the decay rate. Then the effects of off-diagonal damping may be significant. There can also be some level-shifts associated with off-diagonal damping [16], but we will neglect these here.

The beat frequency can be determined from the eigenvalues of the master equation and is found to be [18,17]

$$\omega_b = \mathrm{Re}\sqrt{[(\omega_1-\omega_2)-i(\gamma_1-\gamma_2)/2]^2-\gamma_1\gamma_2}. \tag{5}$$

If the two decay rates are equal, $\gamma=\gamma_1=\gamma_2$, this is simply $\omega_b=\mathrm{Re}\sqrt{(\omega_1-\omega_2)^2-\gamma^2}$.

As the transition operator corresponds to the creation of a photon, which is then subsequently observed, we can formally write the detected intensity of the fluorescence radiation as

$$I(t)\propto \mathrm{Tr}\,[(\sqrt{\gamma_1}\sigma_1^+ + \sqrt{\gamma_2}\sigma_2^+)(\sqrt{\gamma_1}\sigma_1^- + \sqrt{\gamma_2}\sigma_2^-)\rho(t)] \tag{6}$$

and here we define $I(t)$ such that,

$$I(t)=\langle J^\dagger J\rangle = \gamma_1\rho_{11}+\gamma_2\rho_{22}+2\sqrt{\gamma_1\gamma_2}\ \mathrm{Re}\ \rho_{12}, \tag{7}$$

where the brackets mark a quantum statistical average, and thus the signal is given in terms of the system density matrix ρ_{ij}, where the diagonal elements describe the state populations, and the off-diagonal elements describe the coherences between the states.

In the simplest Weisskopf-Wigner theory of decay one simply postulates an exponential decay for the upper state amplitudes C_j [19]. In the case of a quantum beat three-level system we must only take into account the different frequencies of those amplitudes so that [10]

$$C_j(t)=C_j(0)\exp(-\gamma_j t/2 - i\omega_j t). \tag{8}$$

As a result, the populations and the off-diagonal elements of the density matrix all decay exponentially. Although we can include the effects of off-diagonal damping (the coupling of coherences to populations), we neglect these in Eq. (8). Thus Eq. (8) represents a model of *independent exponential decay* for the two states. This model then yields a quantum beat signal (in the dipole approximation) of

$$I(t)\propto|\sqrt{\gamma_1}C_1(t)+\sqrt{\gamma_2}C_2(t)|^2. \tag{9}$$

Then if the decay rates are equal we obtain

$$I(t)\propto e^{-\gamma t}\{1+\cos[(\omega_2-\omega_1)t]\}, \tag{10}$$

and the beat frequency is clearly $\omega_b=\omega_2-\omega_1$. This result differs from the one given in Eq. (5) because of the presence of off-diagonal damping terms in the master equation (1). We note, however, that ω_b in Eq. (5) will approach $\omega_1-\omega_2$ when $(\omega_1,\omega_2)\gg(\gamma_1,\gamma_2)$. This limit is discussed further in Sec. III.

B. Molecular quantum beats

The molecular case is more complex because the system contains an extra degree of freedom: the molecular coordinate(s). Here we confine our attention to a single molecular coordinate that will be denoted by x. Then the Hamiltonian for the molecular system is given by

$$H_0=-\frac{\hbar^2}{2m}\frac{\partial^2}{\partial x^2}\,\mathcal{I}+\begin{bmatrix} U_1(x) & V_1(t) & 0 \\ V_1(t) & U_0(x) & V_2(t) \\ 0 & V_2(t) & U_2(x)\end{bmatrix}, \tag{11}$$

where now $U_0(x)$, $U_1(x)$, and $U_2(x)$ are the spatially dependent electronic potentials for the molecule, and $\mathcal{I}$ is the corresponding identity matrix. The couplings with the laser pulse are given by $V_1(t)$ and $V_2(t)$, and are assumed not to be spatially dependent. The main change, compared to the atomic Hamiltonian, Eq. (3), is the inclusion of the kinetic term with the mass m. However, with this modified Hamiltonian the master equation (1) still governs the evolution of the density matrix. We have now taken into account the excitation of the system, the dynamical evolution, and spontaneous decay. The density matrix depends on the spatial coordinate x as well as the energy state j. That is, the elements of $\rho(t)$ are $\rho_{jj'}(x,x',t)$.

We will see in Sec. III and in Sec. IV that it is not always necessary to solve the full master equation (1) for the molecular problem. The technique of optical potentials, and the utilization of Gaussian wave packets, provide approaches that we will examine in the next sections. However, if we are interested in the ground-state wave-packet dynamics, or if the time taken for the excitation of the pulse is nonnegligible, we must solve Eq. (1). This is a nontrivial task if we try to solve the system numerically by discretization of the density matrix in space and time. The problem is the large memory occupied by the representation of the density matrix [2,20]. This can be drastically reduced by utilizing the Monte Carlo wave-function technique [21]. We have implemented it in the standard way [2,8,20]. Using the transition operator J, Eq. (2), we first determine the probability of photon emission from both upper states during a short time step Δt, that is,

$$\Delta P=\Delta t\langle\Psi|J^\dagger J|\Psi\rangle. \tag{12}$$

Then we obtain a random number r between 0 and 1 and do one of *two* things. If $r<\Delta P$ we perform a transition from the upper states to the ground state (a quantum jump) so that

$$|\Psi\rangle\rightarrow\frac{J|\Psi\rangle}{\sqrt{\langle\Psi|J^\dagger J|\Psi\rangle}}. \tag{13}$$

However, if $r>\Delta P$, there will not be any transition, and instead the system evolves with the non-Hermitian operator

$$\begin{aligned} H_{\mathrm{eff}} &= H_0-\frac{i\hbar}{2}J^\dagger J \\ &= H_0-\frac{i\hbar}{2}[\sqrt{\gamma_1}\sigma_1^+ + \sqrt{\gamma_2}\sigma_2^+][\sqrt{\gamma_1}\sigma_1^- + \sqrt{\gamma_2}\sigma_2^-]. \end{aligned} \tag{14}$$

The non-Hermitian operator $H_{\rm eff}$ can also be written in a matrix form as

$$H_{\rm eff}=H_0-\frac{i\hbar}{2}\begin{bmatrix}\gamma_1 & 0 & \sqrt{\gamma_1\gamma_2}\\ 0 & 0 & 0\\ \sqrt{\gamma_1\gamma_2} & 0 & \gamma_2\end{bmatrix}. \tag{15}$$

This clearly shows diagonal damping terms γ_1,γ_2 and off-diagonal damping terms $\sqrt{\gamma_1\gamma_2}$. The evolution with $H_{\rm eff}$ is performed in a numerical implementation where we discretize the spatial wave functions. Since the system Hamiltonian is now non-Hermitian, we need to renormalize our wave function after each time step. The operator $H_{\rm eff}$ implies that for the wave-function components given by

$$\Psi=\begin{pmatrix}\Psi_1(x,t)\\ \Psi_0(x,t)\\ \Psi_2(x,t)\end{pmatrix} \tag{16}$$

we obtain the partial differential equations

$$\begin{aligned}
i\hbar\frac{\partial}{\partial t}\Psi_0(x,t)&=\left\{-\frac{\hbar^2}{2m}\frac{\partial^2}{\partial x^2}+U_0(x)\right\}\Psi_0(x,t)\\
&\quad+V_1(t)\Psi_1(x,t)+V_2(t)\Psi_2(x,t),\\
i\hbar\frac{\partial}{\partial t}\Psi_1(x,t)&=\left\{-\frac{\hbar^2}{2m}\frac{\partial^2}{\partial x^2}+U_1(x)-\frac{i\hbar}{2}\gamma_1\right\}\Psi_1(x,t)\\
&\quad+V_1(t)\Psi_0(x,t)-\frac{i\hbar}{2}\sqrt{\gamma_1\gamma_2}\Psi_2(x,t),\\
i\hbar\frac{\partial}{\partial t}\Psi_2(x,t)&=\left\{-\frac{\hbar^2}{2m}\frac{\partial^2}{\partial x^2}+U_2(x)-\frac{i\hbar}{2}\gamma_2\right\}\Psi_2(x,t)\\
&\quad+V_2(t)\Psi_0(x,t)-\frac{i\hbar}{2}\sqrt{\gamma_1\gamma_2}\Psi_1(x,t).
\end{aligned} \tag{17}$$

Despite the complications introduced by the decay factors, these coupled partial differential equations can be solved by using the Crank-Nicholson numerical method (used here) or other methods [2]. We note that even in the absence of jumps we have effects from off-diagonal damping. The above steps Eqs. (12)–(14) are repeated for many short time steps to form the stochastic trajectory for the wave function. However, to obtain meaningful results we must obtain many trajectories to form an ensemble. Then the ensemble averages for the observables will approach the values that would be obtained by direct integration of the density matrix master equation (1) with the Hamiltonian H_0, Eq. (11).

We note here that the time step, Δt, used in the Monte Carlo method, e.g., in Eq. (12), need not be the same as the time steps used to integrate Eq. (17). This may be desirable if the decay rates and potentials (or couplings) have rather different time scales, because it enables us to carry out fewer tests, and allows us to rely less on very small numbers from the random number generator.

Finally, we can see that the beat signal follows very naturally from the probability of spontaneous emission in unit time. From Eq. (12) we obtain the same result found in Eq. (7), but this time the coherence ρ_{12} is evaluated as

$$\langle 1|\rho|2\rangle\equiv\left\langle\int dx\Psi_1^*(x,t)\Psi_2(x,t)\right\rangle. \tag{18}$$

Here we have used the brackets to mark the ensemble average. Likewise the populations ρ_{11} and ρ_{22} are simply $\langle 1|\rho|1\rangle$ and $\langle 2|\rho|2\rangle$, respectively.

III. STANDARD QUANTUM BEAT REGIME

We have already pointed out that the result from independent exponential decay, Eq. (8), is not actually a solution of the master equation (1) although the beat signal from the exponential decay treatment approaches the master equation result (5) in the limit $(\omega_1,\omega_2)\gg(\gamma_1,\gamma_2)$. This arises because in this limit we can perform a type of secular approximation which involves neglecting the off-diagonal damping. In this limit the master equation (1) will become

$$\begin{aligned}
\frac{d}{dt}\rho&=-\frac{i}{\hbar}[H_0,\rho]-\frac{\gamma_1}{2}(J_1^\dagger J_1\rho+\rho J_1^\dagger J_1-2J_1\rho J_1^\dagger)\\
&\quad-\frac{\gamma_2}{2}(J_2^\dagger J_2\rho+\rho J_2^\dagger J_2-2J_2\rho J_2^\dagger),
\end{aligned} \tag{19}$$

where the decay is now into two separate channels. Each decay channel has a ''jump operator'':

$$\begin{aligned}
J_1&=\sqrt{\gamma_1}\sigma_1^-,\\
J_2&=\sqrt{\gamma_2}\sigma_2^-.
\end{aligned} \tag{20}$$

We could construct a wave-function simulation for this master equation but, in fact, *if* we are only interested in the upper states of the system this is not necessary. (Note that to evaluate the beat signal Eq. (7) we only need information about coherence and populations on the upper states 1 and 2.) We can use the technique of complex potentials [8,22] where the time evolution of the system is governed by an operator similar to $H_{\rm eff}$ in Eq. (14), but without the off-diagonal damping. Thus we will obtain the coupled differential equations [see Eq. (17)]

$$\begin{aligned}
i\hbar\frac{\partial}{\partial t}\Psi_1(x,t)&=\left\{-\frac{\hbar^2}{2m}\frac{\partial^2}{\partial x^2}+U_1(x)-\frac{i\hbar}{2}\gamma_1\right\}\Psi_1(x,t),\\
i\hbar\frac{\partial}{\partial t}\Psi_2(x,t)&=\left\{-\frac{\hbar^2}{2m}\frac{\partial^2}{\partial x^2}+U_2(x)-\frac{i\hbar}{2}\gamma_2\right\}\Psi_2(x,t),
\end{aligned} \tag{21}$$

which apply after the duration of the excitation pulse. However, unlike the implementation the Monte Carlo wave function simulation described in Eqs. (12)–(14), here we *do not* renormalize the wave functions so that they will decay.

This approach neglects any possibility of reexcitation of the population that has decayed back to the ground state, but provided the excitation pulse is short enough this is a reason-

able approximation. This means that for the duration of the excitation pulse *only* we may implement the equations:

$$i\hbar\frac{\partial}{\partial t}\Psi_0(x,t)=\left\{-\frac{\hbar^2}{2m}\frac{\partial^2}{\partial x^2}+U_0(x)\right\}\Psi_0(x,t)+V_1(t)\Psi_1(x,t)+V_2(t)\Psi_2(x,t),$$

$$i\hbar\frac{\partial}{\partial t}\Psi_1(x,t)=\left\{-\frac{\hbar^2}{2m}\frac{\partial^2}{\partial x^2}+U_1(x)\right\}\Psi_1(x,t)+V_1(t)\Psi_0(x,t), \tag{22}$$

$$i\hbar\frac{\partial}{\partial t}\Psi_2(x,t)=\left\{-\frac{\hbar^2}{2m}\frac{\partial^2}{\partial x^2}+U_2(x)\right\}\Psi_2(x,t)+V_2(t)\Psi_0(x,t).$$

Note also that as the decayed excited states population leaves the 1–2 system in this model, instead of being returned back to the ground state, we cannot get the time evolution of the ground state correctly. In other words, this approach is merely the independent exponential decay treatment taking into account the internal dynamics of the molecular wave packets. However, a clear advantage of this model is that no ensemble averaging is needed, because ρ_{11}, ρ_{22}, and ρ_{12} can be found from the wave-function components as $\rho_{ij}=\Psi_i\Psi_j^*$. Of course, situations arise where this approach is not adequate, and we cannot use it if we are interested in the ground-state dynamics (as is sometimes the case for cold collisions). Then we have to use a master equation approach and a Monte Carlo simulation.

IV. NUMERICAL RESULTS

In the cases that we have studied we can see that there are essentially two major contributions of wave-packet effects to the quantum beat signal. The first effect arises from the separation of wave packet trajectories on the two upper state surfaces. As the wave packets separate the overlap of the two packets decreases and then there is a reduction in the amplitude of the coherence ρ_{12}, Eq. (18). This will then modify the amplitude modulation of the quantum beats. The second effect arises from the fact that as the wave packets on the upper state surfaces evolve in different potentials, there is a time varying energy difference between them. As a result the beat frequency varies in time. We have selected two highly simplified potential surface models in order to study these effects. In addition we have also looked into a situation where the off-diagonal damping should be non-negligible, and indeed we find that it has a small effect in the particular model situation that we have investigated.

In order to solve Eq. (17) numerically we have used the standard scaling presented in Refs. [5,23], i.e., $x\rightarrow x/x_s$, $t\rightarrow t/t_s$, $U_j\rightarrow U_j/v_s$, $V_j\rightarrow V_j/v_s$, where $\hbar t_s=2mx_s^2$ and $v_s=\hbar/t_s$. This scaling corresponds to setting $\hbar=1$ and $m=1/2$, and transforms all parameters and variables into dimensionless quantities. Finally, to avoid numerical integration of quantities evolving at optical frequencies, we change to a basis where the rapid (optical) frequencies in Ψ_1,Ψ_2 are transformed away with equivalent energy subtracted from the potentials U_1,U_2.

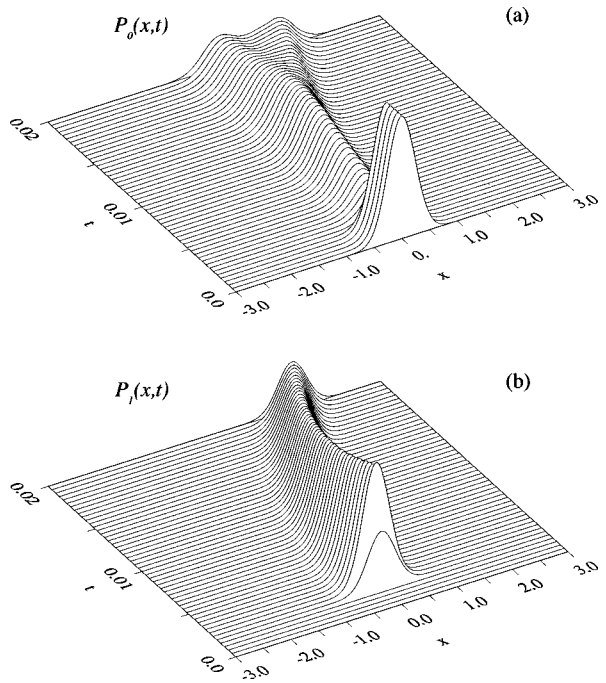

FIG. 2. The components of the wave packet for (a) the ground state 0, (b) the excited state 1. The potentials used in the model are linear $U_j(x)=\Delta_j+\lambda_j x$ with $\lambda_0=0$, $\lambda_1=5000$, and $\lambda_2=4000$ (in scaled units). The detunings are $\Delta_0=0$, $\Delta_1=-5000$, and $\Delta_2=5000$. Thus potentials for the upper states are diverging as the excited state wave packets gain positive momentum and move accordingly. The exciting pulse has a hyperbolic secant profile with a width of 0.001 and peak height of 500. The decay rates are $\gamma_1=\gamma_2=50$. The ensemble averaged results contain 5000 samples and 500 spatial points were used in the numerical integration. The wave packet has width 0.25 and starts in the ground state 0.

A. Linearly separating energy states

In this first model we have used simple linear potentials so that if the wave packets can be treated as approximately classical particles, the energy difference is increasing quadratically in time. As a result the beat frequency should increase quadratically too (as long as we do not approach a curve crossing). The potentials used in the model are

$$U_j(x)=\Delta_j+\lambda_j x, \tag{23}$$

where the slopes of the potentials are (in scaled units): $\lambda_0=0$, $\lambda_1=5000$, $\lambda_2=4000$. The detunings are $\Delta_0=0$, $\Delta_1=-5000$, and $\Delta_2=5000$. Thus the potentials for the upper states are diverging as the excited-state wave packets gain positive momentum and move accordingly. The exciting pulse has a hyperbolic secant profile with a width of 0.001 and peak height of 500. The decay rates are $\gamma_1=\gamma_2=50$ and the ensemble-averaged results contain 5000 samples.

The excitation of both the excited states is initially about 40% because a very short excitation pulse with a suitable area is used. Figure 2 shows the probability densities $P_j(x,t)=|\Psi_j(x,t)|^2$ for $j=0$ (a) and $j=1$ (b); the case $j=2$ is omitted as it is very similar to the case $j=1$. Both

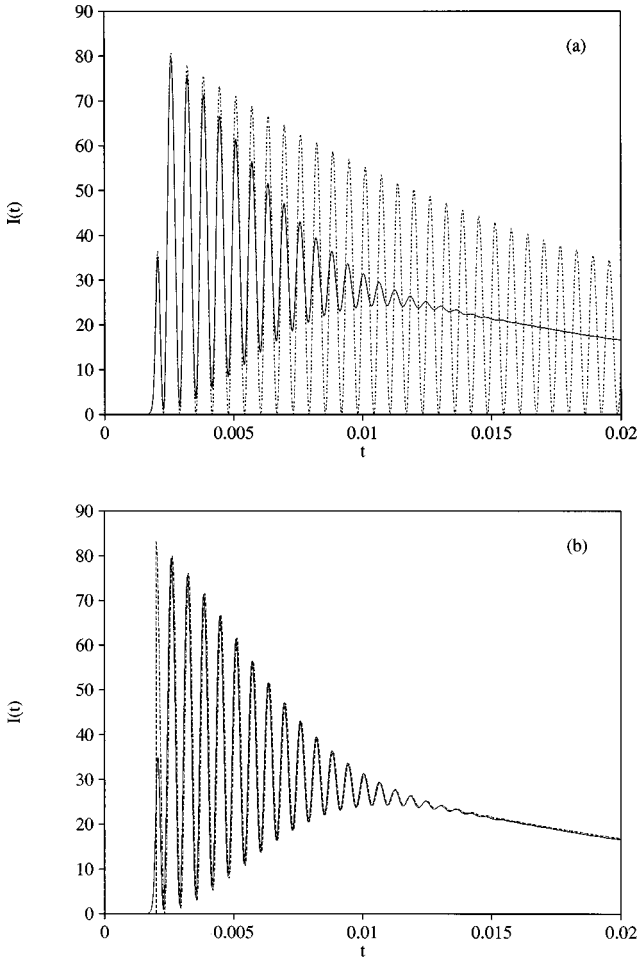

FIG. 3. Quantum beat signal for the parameters of Fig. 2. The solid curve in both (a) and (b) shows the numerically calculated beat signal, the dotted line in (a) shows the signal from a system with fixed energy difference. The dashed line in (b) shows the semiclassical exponential decay result given by Eqs. (30) and (31).

excited-state wave packets accelerate, spread, and decay back down to the ground state. The ground-state wave packet becomes very spread out because it contains contributions from both upper state trajectories and the ground-state population that was not removed by the pulse.

The beat signal in Fig. 3(a) (solid curve) shows a slight frequency chirp because of the time-dependent increase in energy-state separation. However, the modulation decreases quite rapidly in time. This is because of the increasing separation of the wave packets, which reduces their overlap and the possibility for beats. For comparison we have also plotted the result of a density matrix calculation [dotted curve in Fig. 3(a)], with no wave packets, and for an energy difference that is fixed in time at the initial value. In this case the signal does not wash out so rapidly, and the requirement of spatial overlap does not apply here. The dephasing of the wave packet beat signal can be clearly seen.

In order to provide a more quantitative analysis we consider a simple model where the excitation process is presumed to place two perfectly Gaussian wave packets on the excited states 1 and 2. Then if we (initially) neglect the decay process, the time-dependent evolution of the wave packet on state j ($j=1,2$) is given by [24]

$$\Psi_j(x,t)=\frac{\sqrt{\sigma_0}}{(2\pi)^{1/4}\tilde{\sigma}(t)}\exp\left[-\frac{[x-x_j(t)]^2}{[2\tilde{\sigma}(t)]^2}+\frac{ip_j(t)}{\hbar}[x-x_j(t)]+\frac{i\lambda_j^2t^3}{3m\hbar}-\frac{iE_jt}{\hbar}\right], \quad (24)$$

where the wave packet starts at position x_0 with no momentum and the classical trajectory of the wave packet is

$$x_j(t)=x_0-\lambda_jt^2/(2m), \quad (25)$$

$$p_j(t)=-\lambda_jt. \quad (26)$$

The classical energy is $E_j=\Delta_j+\lambda_jx_0$. Then on both states 1 and 2 the initial width of the wave packet is σ_0 and the parameter $\tilde{\sigma}(t)$ is defined as

$$\tilde{\sigma}(t)=\sqrt{\sigma_0^2+it\hbar/(2m)}. \quad (27)$$

We note that from the wave packet (24) we can determine the time-dependent width of the packet as

$$\sigma(t)=\sigma_0\sqrt{1+(t/\tau_d)^2}, \quad (28)$$

where we have defined a time scale τ_d for the spreading of the wave packet:

$$\tau_d=\frac{2m\sigma_0^2}{\hbar}. \quad (29)$$

Then by combining two of the wave packets (24), one with amplitude a_1 on state 1, and the other with amplitude a_2 on state 2, we may compute the time-dependent overlap as

$$O_{12}(t)=a_1^*a_2\exp\left[i(E_1-E_2)t/\hbar-\frac{(\lambda_1-\lambda_2)^2\sigma_0^2}{2\hbar^2}t^2-i\frac{(\lambda_1^2-\lambda_2^2)}{12m\hbar}t^3-\frac{(\lambda_1-\lambda_2)^2}{32m^2\sigma_0^2}t^4\right]. \quad (30)$$

The exponential contains three terms of which the two imaginary terms will contribute to the beats (when we consider decay) and the two real terms will affect the envelope of the beats. In fact the last term in Eq. (30) arises simply from the overlap of two packets, of fixed width σ_0 separating on the trajectories (26). This last term dominates Eq. (30) at large times, but note that the two packets spread as well, according to Eq. (28)—this partly explains the second term in Eq. (30). The third term arises from the energy chirping of the wave packets and takes place on a time scale τ_d faster than the overlap decay in the last term. The rate of change of this term, i.e., the instantaneous beat frequency, increases quadratically in time as mentioned at the start of this section. On short time scales the second term in Eq. (30) dominates the envelope decay until we approach the spreading time scale τ_d. This is because it is found from the last term in Eq. (30) by multiplication with the factor $(\tau_d/2t)^2$. Finally, the first term in Eq. (30) arises simply from the initial energy difference and contributes to the oscillations in the beat signal. All these terms will affect the beat signal, so conversely,

if we can measure some, or all of these parameters from the beat signal we can obtain considerable information (e.g., the two slopes) in the region over which two potential energy surfaces are linear.

To take some account of the decay process, we may simply adopt the exponential decay approach, neglecting the off-diagonal damping, so that, for equal decay rates γ,

$$\rho_{12}(t)=O_{12}(t)\exp(-\gamma t),$$
$$\rho_{11}(t)=|a_1|^2\exp(-\gamma t), \tag{31}$$
$$\rho_{22}(t)=|a_2|^2\exp(-\gamma t),$$

and then the beat signal is given by Eq. (7). For the example of Fig. 3 we have plotted the resulting signal as the dashed curve in Fig. 3(b) and we see that there is an extremely good fit except near the region of excitation. Obviously this simple model cannot take into account the details of the excitation process, and this is the main reason for the discrepancies.

B. Beats from a model with oscillator potentials

Many molecular systems have low-lying states that approximate anharmonic oscillators. Because these oscillator potentials are displaced with respect to each other the wave packets in the excited states have different amplitudes of oscillation, which strongly affects the resulting quantum beats. For our numerical calculations we have used the harmonic potentials

$$U_j(x)=\Delta_j+\tfrac{1}{2}m\Omega(x-x_j)^2, \tag{32}$$

where in this run the period is $\pi/8$ (in scaled units) and $x_0=0.0$, $x_1=0.5$, $x_2=1$. The exciting pulse has a hyperbolic profile with a width of 0.001 and peak height of 500. The decay rates are $\gamma_1=\gamma_2=3.0$ and the ensemble averaged results contain 1000 samples. The excitation of both the excited states is about 50% because again a very short excitation pulse with a suitable area is used. Figure 4 shows the probability densities $P_j(x,t)$ for $j=0,1,2$. Both excited state wave packets oscillate and decay, thus slowly repopulating the electronic ground state of the system; note that the electronic ground state becomes vibrationally excited as population returns.

The beat signal presented in Fig. 5 (solid curve) shows revivals when the two excited-state wave packets return to near their original positions, i.e., when their spatial overlap is at maximum (note that potentials are harmonic and have the same oscillator frequency). The signal is frequency modulated because of the time-dependent energy shift. This can be clearly seen by comparing the signal to the dotted curve in Fig. 5(a), which shows the beat signal from a system with static energy difference fixed at the initial value of the wave-packet system.

As in the linear case, Sec. IV A, we can pursue a simple model with exponential decay (neglecting off-diagonal damping), and impulsive excitation (neglecting the finite time of excitation). With the harmonic potentials (32) the time-dependent overlap of the excited-state wave packets, in the absence of dissipation, is [as defined in Eq. (30)]

$$O_{12}(t)=a_1^*a_2\exp\left\{i(\Delta_1-\Delta_2)t/\hbar+\frac{1}{(2\sigma_0)^2}\times[-2x_{12}^2\sin^2(\Omega t/2)-2ix_{12}(x_0-\overline{x})\sin\,\Omega t]\right\}, \tag{33}$$

where the separation of the oscillators is $x_{12}=x_1-x_2$ and their mean position is $\overline{x}=(x_1+x_2)/2$. Then the approximate beat signal in the presence of decay is given by Eqs. (7) and (31) as

$$I(t)=\gamma\left\{|a_1|^2+|a_2|^2+2|a_1a_2|\exp\left(\frac{-2x_{12}^2\sin^2(\Omega t/2)}{(2\sigma_0)^2}\right)\times\cos\left[\phi+(\Delta_1-\Delta_2)t/\hbar-\frac{2x_{12}(x_0-\overline{x})\sin\,\Omega t}{(2\sigma_0)^2}\right]\right\}, \tag{34}$$

where ϕ is the phase angle of $a_1^*a_2$. Figure 5(b) shows the beat signal (34) as the dashed line that provides a good fit to the exact numerical result (solid line).

C. Strong effects of off-diagonal damping

As we have seen in Eq. (5) the effects of the off-diagonal terms in the master equation do not have a significant effect unless the energy difference between the two upper states is less than, or comparable to, the decay rate from the upper states. This situation will certainly arise if the two excited states cross at some value of the molecular coordinate x. Then if a wave packet travels through that ''crossing'' we will find that we have a momentary coupling of the two excited-state energy states. This takes place even though there is no *direct* coupling between the two excited states, that is, there is no coupling, excitation, or pumping between the excited states in the Hamiltonian (11). However, there is an indirect coupling that may be regarded as due to the reabsorption by one transition of the radiation by another, nearly resonant, transition in the system. The effect is clearly seen if the wave packet starts entirely on one of the excited states and then traverses the crossing. Because of the off-diagonal damping, part of the wave packet is transferred to the other excited state nonadiabatically. In order to perform numerical calculations, we could use the quantum Monte Carlo procedure outlined in Eqs. (12)–(17). However, if we are not interested in the ground-state dynamics, this approach is time consuming and not necessary. The optical potential approach as presented in Eq. (21) would not be appropriate here because it neglects the effects of off-diagonal damping. However, we can include the effects of off-diagonal damping in an approach based on optical potentials by utilizing Eqs. (17) for the excited states in the absence of an excitation pulse. That is, we integrate the equations:

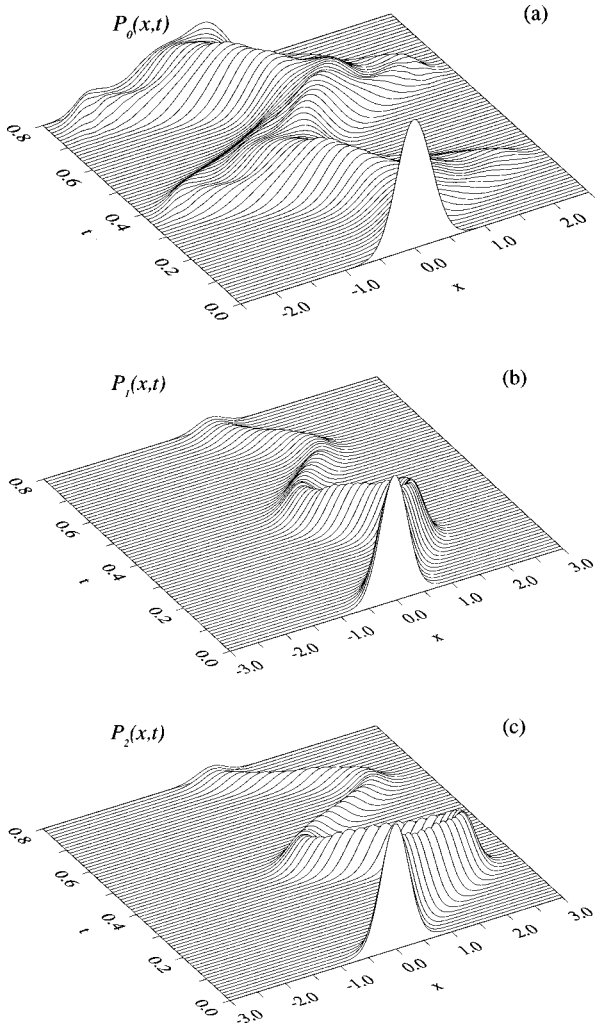

FIG. 4. Here we show the components of the wave packet for (a) the ground state 0, (b) the excited state 1, and (c) the excited state 2. The corresponding potentials are $U_j(x)=\Delta_j+\frac{1}{2}m\Omega(x-x_j)^2$, where $\Omega=\pi/8$ (in scaled units) and $x_0=0.0$, $x_1=0.5$, $x_2=1$. The energy separation of the potentials is given by Δ_j's, which have the values $\Delta_0=0.0$, $\Delta_1=-500$, and $\Delta_2=500$. The exciting pulse has a hyperbolic profile with a width of 0.001 and peak height of 500. The decay rates are $\gamma_1=\gamma_2=3.0$. The ensemble averaged results contain 1000 samples and there are 2000 spatial points.

$$i\hbar\frac{\partial}{\partial t}\Psi_1(x,t)=\left\{-\frac{\hbar^2}{2m}\frac{\partial^2}{\partial x^2}+U_1(x)-\frac{i\hbar}{2}\gamma_1\right\}\Psi_1(x,t)$$
$$-\frac{i\hbar}{2}\sqrt{\gamma_1\gamma_2}\Psi_2(x,t),$$

$$i\hbar\frac{\partial}{\partial t}\Psi_2(x,t)=\left\{-\frac{\hbar^2}{2m}\frac{\partial^2}{\partial x^2}+U_2(x)-\frac{i\hbar}{2}\gamma_2\right\}\Psi_2(x,t)$$
$$-\frac{i\hbar}{2}\sqrt{\gamma_1\gamma_2}\Psi_1(x,t). \tag{35}$$

Figure 6 gives an example of this type of process and shows the population of the excited state 2 when a wave packet initially on a flat state 1 passes through a crossing of the upper excited states, i.e., at the intersection with the sloping

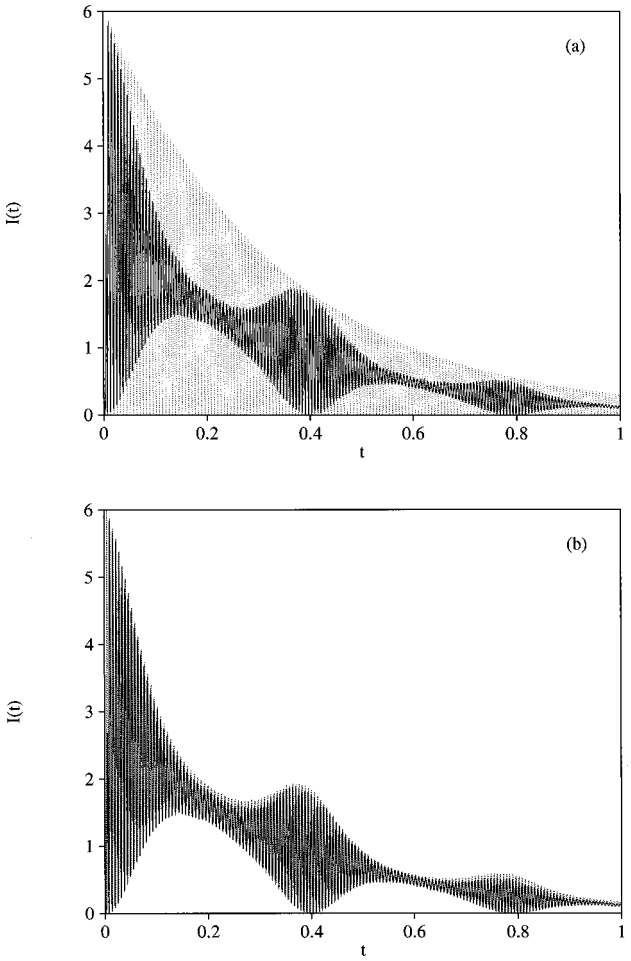

FIG. 5. Quantum beat signal for the parameters of Fig. 4. The solid curve in both (a) and (b) shows the numerically calculated beat signal. The dotted line in (a) shows the signal from a system with fixed energy difference, and the dashed line in (b) shows the curve given by Eqs. (34) with $\phi=0$.

potential 2. We see that the population on state 2 abruptly rises as the wave packet approaches the crossing, thereafter there are oscillations, because of nonadiabatic transitions and the temporary creation of coherence between the two excited states. The oscillations, and the population on state 2 (and state 1), then all die out because of the straightforward, diagonal part of the damping.

Although, in the end, all of the excited-state population ends up on the ground state, the off-diagonal damping, and the transfer of population to state 2 (in Fig. 6), does delay the arrival of population on the ground state. Thus the rise in the ground-state population is interrupted by a hole during, and after, the transit of the wave packet through the crossing. The momentum distribution on the ground state can be strongly affected by the off-diagonal damping effect. For example, with the configuration of states in Fig. 6 the wave packet on excited state 1 is not accelerated and its momentum distribution is transferred to the ground state. However, because of off-diagonal damping, some of the wave packet is transferred to state 2, where it can decelerate before eventually decaying back to the ground state. In this case the average momentum of the ground state can be affected by the off-diagonal damping in the manner demonstrated in Ref. [20].

We know that in simple dynamical curve crossings in-

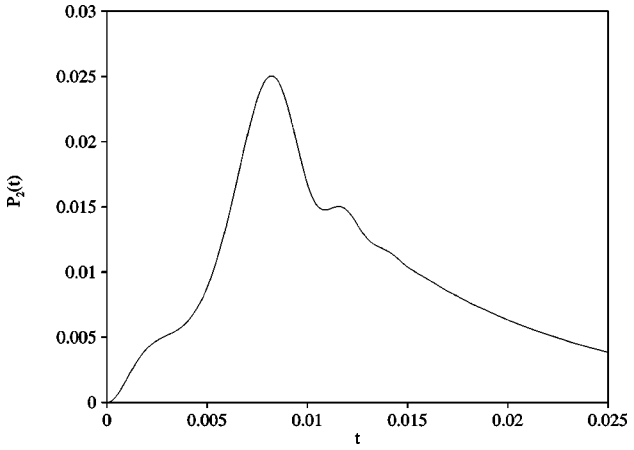

FIG. 6. The population of the excited state 2 when a wave packet on state 1 traverses a crossing of the two excited states. The potentials used in the model are of the linear form (23): $U_j(x) = \Delta_j + \lambda_j x$. However, the ground state 0 and the initial state 1 are flat, $\lambda_0 = \lambda_1 = 0$, there are no detunings, $\Delta_0 = \Delta_1 = \Delta_2 = 0$, and only state 2 has a slope, $\lambda_2 = 1000$. The decay rates are $\gamma_1 = \gamma_2 = 100$ and the ensemble-averaged results contain 1000 samples. The number of spatial points is 3000. There is no excitation pulse here; the initial Gaussian wave packet, with width 0.25, has been simply placed on state 1 with the center position $x = -1.75$ with initial momentum $p = 200$.

volving linear potentials the population transfer $P_{\rm tr}$ is given by the Landau-Zener result

$$P_{\rm tr} = 1 - \exp\left(-2\pi \frac{V^2}{\hbar v_C (\lambda_i - \lambda_j)} \right), \tag{36}$$

where v_C is the mean momentum of the wave packet at the crossing, V is the coupling between states i and j, and $\lambda_{i,j}$ are the slope parameters for the two coupled linear potentials [2,25,26]. We can try to apply the Landau-Zener result to our situation as well, with $V = \sqrt{\gamma_1 \gamma_2}$. Then it is easy to see why the phenomenon described above is difficult to see in practice. The time scale for the wave-packet motion must be fast compared to the time scale of decay, so that there is a nonnegligible amount of excited population around when the wave packet reaches the crossing. However, there must be enough time for the dynamics on the different excited-state trajectories to affect the properties of the wave-packet component before the decay back to the ground state. Thus fast wave packets would be appropriate, but then, as Eq. (36) implies, the transfer probability due to the off-diagonal decay is very small. Thus in general we expect that dynamical population transfer due to the off-diagonal coupling in quantum beat systems does not have any major role in femtochemistry. It may, however, have some impact on cold collision studies, where we encounter large sets of laser-coupled, close-lying partial wave states.

V. CONCLUSION

In this paper we have investigated how to study quantum beats in wave-packet systems using the Monte Carlo wave-function technique. We have explicitly shown that the master equation and thus the equations used in the Monte Carlo approach for a quantum beat system are conceptually different from the equations describing systems where the spontaneously emitted photons allow transition routes to be identified. When the linewidths of the excited states are smaller than their energy differences, then the structures (but not the interpretations) of the equations become equal—this has led to slightly incorrect description of quantum beats in the literature in the past.

In addition to the exact description of the framework for studying the quantum beat effects in wave-packet dynamics we have used examples to look into the possible wave-packet phenomena that may arise in quantum beat systems. The simplicity of our examples has allowed us to compare our results with simple models based on combining uncoupled wave-packet evolution on potential surfaces with the Weisskopf-Wigner model for the spontaneous emission, i.e., with a model of independent exponential decay from the two excited states. The proper quantum beat equations have off-diagonal damping, and we have also studied its role in wave-packet dynamics involving excited-state potential surface crossings. Although it seems that off-diagonal damping is not an important phenomenon in molecular femtochemistry processes, it may need to be taken into account in cold collision systems.

ACKNOWLEDGMENTS

This work was supported by the United Kingdom Engineering and Physical Sciences Research Council, and the Academy of Finland. The authors thank Bryan Dalton, Peter Knight, and Stig Stenholm for enlightening remarks. B.M.G. acknowledges the hospitality of the Research Institute for Theoretical Physics and the Helsinki Institute of Physics at the University of Helsinki.

[1] A.H. Zewail, Science **242**, 1645 (1988); M. Gruebele and A.H. Zewail, Phys. Today **43** (5), 24 (1990); A.H. Zewail, Sci. Am. **263(12)**, 40 (1990); *The Chemical Bond*, edited by A.H. Zewail (Academic Press, San Diego, 1992); A.H. Zewail, J. Phys. Chem. **97**, 12 427 (1993).

[2] B.M. Garraway and K.-A. Suominen, Rep. Prog. Phys. **58**, 365 (1995).

[3] J. Macek, Phys. Rev. A **1**, 618 (1970); J.N. Dodd and G.W. Series, in *Progress in Atomic Spectroscopy*, Pt. A, edited by W. Hanle and H. Kleinpoppen (Plenum, New York, 1978), p. 639; S. Haroche, *High-resolved Laser Spectroscopy*, in Topics in Applied Physics, edited by K. Shimoda (Springer, Berlin, 1976), Vol. 13, p. 253.

[4] B.J. Dalton, J. Phys. B **12**, 2625 (1979); B.J. Dalton, *ibid.* **20**, 251 (1987).

[5] K.-A. Suominen, B.M. Garraway, and S. Stenholm, Phys. Rev. A **45**, 3060 (1992); A. Paloviita, K.-A. Suominen, and S. Stenholm, J. Phys. B **28**, 1463 (1995); A. Paloviita, Opt. Commun. **119**, 533 (1995); A. Paloviita and K.-A. Suominen, Phys. Rev. A **55**, 3007 (1997).

[6] T.J. Dunn, J.N. Sweetser, I.A. Walmsley, and C. Radzewicz, Phys. Rev. Lett. **70**, 3388 (1993).

[7] P.S. Julienne, A.M. Smith, and K. Burnett, Adv. At., Mol., Opt. Phys. **30**, 141 (1993); T. Walker and P. Feng, *ibid.* **34**, 125 (1994); J. Weiner, *ibid.* **35**, 45 (1995); K.-A. Suominen, J. Phys. B **29**, 5981 (1996).

[8] M.J. Holland, K.-A. Suominen, and K. Burnett, Phys. Rev. Lett. **72**, 2367 (1994); Phys. Rev. A **50**, 1513 (1994); P.S. Julienne, K.-A. Suominen, and Y. Band, *ibid.* **49**, 3890 (1994); K.-A. Suominen, M.J. Holland, K. Burnett, and P.S. Julienne, *ibid.* **49**, 3897 (1994); **51**, 1446 (1995); Y.B. Band, I. Tuvi, K.-A. Suominen, K. Burnett, and P.S. Julienne, *ibid.* **50**, R2826 (1994).

[9] K.-A. Suominen, K. Burnett, and P.S. Julienne, Phys. Rev. A **53**, R1220 (1996).

[10] B.W. Shore, *The Theory of Coherent Atomic Excitation* (Wiley, New York, 1990), Vol. 2, Chap 13.8; P. Meystre and M. Sargent III, *Elements of Quantum Optics*, 2nd ed. (Springer-Verlag, Berlin, 1991), Chap. 13.4.

[11] H.J. Andrä, in *Progress in Atomic Spectroscopy*, Pt. B, edited by W. Hanle and H. Kleinpoppen (Plenum, New York, 1978), p. 829.

[12] I.C. Khoo and J.H. Eberly, Phys. Rev. A **14**, 2174 (1976).

[13] S. Stenholm, in *Frontiers in Laser Spectroscopy*, edited by R. Balian, S. Haroche, and S. Liberman, Les Houches Lecture Notes in Physics (North-Holland, Amsterdam, 1977), Vol. XXVII, p. 399.

[14] P.W. Milonni, Phys. Rep., Phys. Lett. **C25**, 1 (1976).

[15] D.A. Cardimona, M.G. Raymer, and C.R. Stroud, Jr., J. Phys. B **15**, 55 (1982).

[16] D.A. Cardimona and C.R. Stroud, Jr., Phys. Rev. A **27**, 2456 (1983).

[17] B.M. Garraway and P.L. Knight, Phys. Rev. A **54**, 3592 (1996).

[18] G.C. Hegerfeldt and M.B. Plenio, Quantum Opt. **6**, 15 (1994); A. Schenzle and R.G. Brewer, in *Proceedings of the 2nd International Conference on Laser Spectroscopy*, Lecture Notes in Physics Vol. 43, edited by S. Haroche and A.C. Pebay-Peroula (Springer-Verlag, Berlin, 1975), p. 420.

[19] V. Weisskopf and E. Wigner, Z. Phys. **63**, 54 (1930).

[20] W.K. Lai, K.-A. Suominen, B.M. Garraway, and S. Stenholm, Phys. Rev. A **47**, 4779 (1993); K.-A. Suominen and B.M. Garraway, *ibid.* **48**, 3811 (1993); W.K. Lai and S. Stenholm, Opt. Commun. **104**, 313 (1994).

[21] H.J. Carmichael, *An Open Systems Approach to Quantum Optics*, Lecture Notes in Physics Vol. m18 (Springer-Verlag, Berlin, 1993); J. Dalibard, Y. Castin, and K. Mølmer, Phys. Rev. Lett. **68**, 580 (1992); K. Mølmer, Y. Castin, and J. Dalibard, J. Opt. Soc. Am. B **10**, 524 (1993); P.L. Knight and B.M. Garraway, in *Quantum Dynamics of Simple Systems*, Proceedings of the 44th Scottish Universities Summer School in Physics, edited by G.-L. Oppo *et al.* (IOP Publishing, Bristol, 1996), p. 199.

[22] H.M.J.M. Boesten, B.J. Verhaar, and E. Tiesinga, Phys. Rev. A **48**, 1428 (1993); H.M.J.M. Boesten and B.J. Verhaar, *ibid.* **49**, 4240 (1994).

[23] B.M. Garraway and S. Stenholm, Phys. Rev. A **46**, 1413 (1992).

[24] M.S. Child, *Semiclassical Mechanics with Molecular Applications* (Oxford University Press, Oxford, 1991).

[25] L.D. Landau, Phys. Z. Sowjetunion **2**, 46 (1932); C. Zener, Proc. R. Soc. London, Ser. A **137**, 696 (1932).

[26] B.M. Garraway and S. Stenholm, Opt. Commun. **83**, 349 (1991).